Forces stabilizing the complex formed between 7-aminoactinomycin D and a DNA hairpin: Solvatochromism and NMR studies.

ARTICLE *in* BIOPHYSICAL JOURNAL · JANUARY 2001

Impact Factor: 3.97

7 AUTHORS, INCLUDING:

Nikolai Vekshin

Russian Academy of Sciences

80 PUBLICATIONS **275** CITATIONS

SEE PROFILE

Alexander E. Kovalev

Christian-Albrechts-Universität zu Kiel

58 PUBLICATIONS **513** CITATIONS

SEE PROFILE

David E Graves

University of Alabama at Birmingham

85 PUBLICATIONS **1,799** CITATIONS

SEE PROFILE

Randy M Wadkins

University of Mississippi

72 PUBLICATIONS **1,519** CITATIONS

SEE PROFILE

Solvatochromism of the Excitation and Emission Spectra of 7-Aminoactinomycin D: Implications for Drug Recognition of DNA Secondary Structures

Nikolai Vekshin,[†] Ivan Savintsev,[†] Alexandr Kovalev,[†] Ruslan Yelemessov,[†] and Randy M. Wadkins*[,‡]

Institute of Cell Biophysics, 142292 Pushchino, Moscow Region, Russian Federation, and Department of Oncology, Johns Hopkins University School of Medicine, Bunting−Blaustein Cancer Research Building 1M90, 1650 Orleans St., Baltimore, Maryland 21231

Received: March 28, 2001; In Final Form: June 17, 2001

The antitumor antibiotic 7-aminoactinomycin D has been previously demonstrated to bind and stabilize transient hairpin structures formed by single-stranded DNA. Those experiments suggested that DNA secondary structures are viable targets for development of novel antitumor or antiviral compounds. Interestingly, when 7-aminoactinomycin D binds to hairpins formed by selected single-stranded DNAs having a high affinity for the drug, the fluorescence quantum yield, average fluorescence lifetime, excitation wavelengths, and emission wavelengths for the drug are significantly different from those observed when it is free in solution or bound to duplex, B-form DNA. This suggests a unique physical chemical environment within certain DNA hairpins that is specifically recognized by the drug. To understand the environmental contribution to the fluorescence properties of the bound drug, we used solvatochromism techniques, whereby 7-aminoactinomycin D fluorescence properties were determined in 20 solvents with known polarization (π), hydrogen bond donor (α), and hydrogen bond acceptor (β) properties. These data reveal solvent hydrogen bonding to 7-aminoactinomycin D in the excited state. Semiempirical molecular orbital methods have been used to calculate the electronic structure of the first singlet excited state of 7-aminoactinomycin D. The calculations indicate the redistribution of electron density in the excited-state involves the oxygen atom attached to carbon 3 of the phenoxazone ring system. Hence, the solvent-dependent changes in fluorescence properties of 7-aminoactinomycin D involve solvent hydrogen bonding to this oxygen. This oxygen is protected from solvent in the binding site for 7-aminoactinomycin D on selected DNA hairpin secondary structures due to the unique chemical environment of this site.

Introduction

There is widespread interest in actinomycin D (AMD) in the biological sciences due to the drug's activity as an antibiotic and as an antitumor agent (reviewed in [42,6]). The drug inhibits transcription in a wide variety of systems [7,17,29,32,43]. In vitro, the drug binds to double-stranded DNA (dsDNA) containing GC sites, and the high affinity and slow dissociation from these DNAs has suggested a mechanism whereby the drug blocks the progression of RNA polymerase along the template DNA, stopping transcription.[24] Although discovered in the 1940s, AMD is still used clinically for the treatment of a number of cancers, including Ewing's sarcoma, Wilms' tumor, and rhabdomyosarcomas.[36]

In several previous reports, AMD has been shown to bind with high affinity to selected single-stranded DNA (ssDNA) sequences, most of which adopt hairpin conformations [39,38,11,41,40,28]. Such binding to ssDNA is the likely mode by which AMD inhibits HIV reverse transcriptase and other DNA polymerases requiring a ssDNA template.[26,4,9,12] Hence, selective targeting of DNA secondary structures such as hairpins by AMD may serve as a model system for development of novel antitumor and/or antiviral agents with similar modes of action, but with higher target selectivity.[37]

The initial investigations into AMD binding to ssDNA were launched partly from the unusual photophysical properties of the drug upon binding to selected ssDNA. The absorption spectrum of AMD bound to ssDNA showed a red (bathochromic) shift relative to the drug free in aqueous buffer.[39,38] This shift was more pronounced than with duplex, dsDNA. However, the most striking difference between the properties of the bound vs free drug was observed using the fluorescent analogue of AMD, 7-aminoactinomycin D (7AAMD; see Figure 3A). This analogue has been shown to bind ssDNA and dsDNA as AMD, and to have identical biological activity as AMD [23,3,5,8,39]. Upon binding of 7AAMD to selected ssDNA sequences, the fluorescence excitation spectrum is shifted to longer wavelengths, whereas there is a large blue (hypsochromic) shift in the emission spectrum.[39,38] Additionally, the quantum yield of the bound vs free drug is strongly enhanced (see Figure 1). These spectral changes are distinct from those previously observed for 7AAMD binding to dsDNA.[5,3]

Interestingly, the enhancement of quantum yield upon binding of 7AAMD to selected ssDNA is correlated with the affinity of 7AAMD for a ssDNA.[41] The more intense the fluorescence of the bound drug, the higher the affinity for the ssDNA. This suggests that the electronic properties of the drug in the binding

* To whom correspondence should be addressed. Phone: (410)-955−8368. Fax: (410)-614−9006. E-mail: rwadkin@jhmi.edu.

[†] Institute of Cell Biophysics, 142292 Pushchino, Moscow Region, Russian Federation.

[‡] Department of Oncology, Johns Hopkins University School of Medicine, Bunting-Blaustein Cancer Research Building 1M90, 1650 Orleans St., Baltimore, Maryland.

10.1021/jp011168p CCC: $20.00
Published on Web 08/14/2001

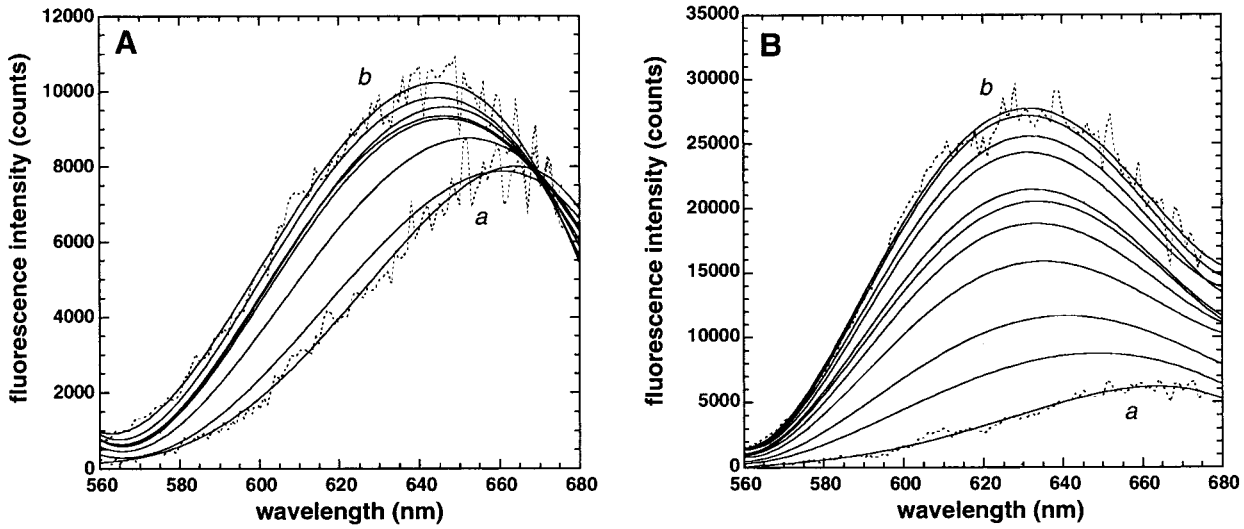

Figure 1. Fluorescence spectral shifts upon binding of 7-aminoactinomycin D to DNA. The corrected emission spectra of 0.3 μM 7-aminoactinomycin D is shown as line *a* in both panels. (A) The emission spectra upon addition of calf thymus DNA. Smoothed fluorescence curves are shown for the addition of 1.5, 6.1, 12.1, 30.3, and (*b*) 60.6 μM (nucleotides) sonicated calf thymus DNA. Actual data before smoothing are shown for curves *a* and *b* as the dashed line. (B) The emission spectra upon addition of the DNA hairpin HP1 (see text). Smoothed fluorescence curves are shown for the addition of 0.05, 0.1, 0.2, 0.3, 0.4, 0.5, 0.75, 1.0, 1.5, and (*b*) 2.0 μM (strands) HP1. Actual data before smoothing are shown for curves *a* and *b* as the dashed line.

site are directly connected to the physical chemical environment responsible for drug recognition. Previously, one of us demonstrated that the source of the enhancement of quantum yield for 7AAMD bound to a ssDNA hairpin resulted from a shift in the fraction of 7AAMD molecules having a longer fluorescence lifetime.[39] The drug in aqueous buffer alone has two components contributing to its fluorescence: one with a fluorescence lifetime of 0.4 ns comprising 89% of the fluorescent species and one with a lifetime of 1.9 ns comprising 11% of the fluorescent species. In the presence of ssDNA, there is a shift in the population of the two species: 48% of the species now has a lifetime of 0.6 ns while 52% has a lifetime of 2.0 ns. Our interpretation of these data is that the solvent and/or electronic environment of the binding site on ssDNA greatly stabilizes the excited state of the 7AAMD.

The fluorescence properties of 7AAMD act as a probe for the nature of the high-affinity binding site for the drug in ssDNA hairpins. To understand how the photophysical properties of 7AAMD are influenced by the environment of the drug, we have made measurements of the solvatochromism of the excitation and emission spectra of 7AAMD in 20 solvents with known polarization/polarizability (π), hydrogen bond donor (α), and hydrogen bond acceptor (β) properties.[15] The resulting linear solvation energy relationship is described in this report, and is interpreted with the aid of semiempirical molecular orbital calculations of the 7AAMD excited state. We describe how our results have been used to understand the binding environment of 7AAMD on ssDNA, and how they have important implications for development of novel compounds to target DNA secondary structures.

Materials and Methods

Materials. Actinomycin D and 7-aminoactinomycin D were purchased from Fluka and used without further purification. The ssDNA named HP1 (5′-AAAAAAATAGTTTTAAATATTTT-TTT-3′; [41]) was purchased from Midland Research Chemical Co. (Midland, Texas) It was synthesized using standard solid-phase technology and purified using ion exchange HPLC. Organic solvents were purchased from standard commercial sources.

Fluorescence Measurements. The steady-state fluorescence excitation and emission spectra and fluorescence polarization of 7AAMD were measured in 20 organic solvents using a SLM-4800 fluorescence spectrometer equipped with Glan−Thompson prisms. Emission spectra were corrected using rhodamine 6 G as a standard. All spectra were than fitted using least-squares methods with one or two Gaussians to obtain excitation and emission peak maximum (and hence, Stokes shift) and peak width at half-height. Polarization measurements were made at the emission maximum.

Fluorescence lifetimes were measured using the phase modulation technique in the SLM-4800, with modulation at 30 MHz (the highest frequency available with this instrument). Consequently, the measured lifetimes are weighted averages. Fluorescence lifetimes were directly measured for 7AAMD in DMSO, H_2O, and D_2O. Lifetimes in other solvents were calculated from the polarization data using the well-known Levshin-Perrin relationship[35]

$$V = \left(\frac{(1/P_0 - 1/3)RT\tau}{(1/P - 1/P_0)\eta} \right) \quad (1)$$

where P is measured polarization, P_0 is the limiting polarization, R is the gas constant, T is absolute temperature, η is the viscosity of the solvent, τ is the fluorescence lifetime in the solvent, and V is the molecular volume of 7AAMD. The limiting polarization value of 0.50 was used[18,35]. The molecular volume for 7AAMD alone determined in H_2O and D_2O was 3510 Å^3 (with corresponding diameter of 5.3 Å) and 3160 Å^3 (diameter 5.2 Å), respectively. We assumed the molecular volume did not change in the other solvents. Solvent viscosity was obtained from standard tables.[22,25]

Linear Solvation Energy Relationships. The peak of the excitation and emission spectra, their widths, and Stokes shifts in different organic solvents can be described with four free parameters using the Kamlet−Taft expression.[15,16,33,14] They are

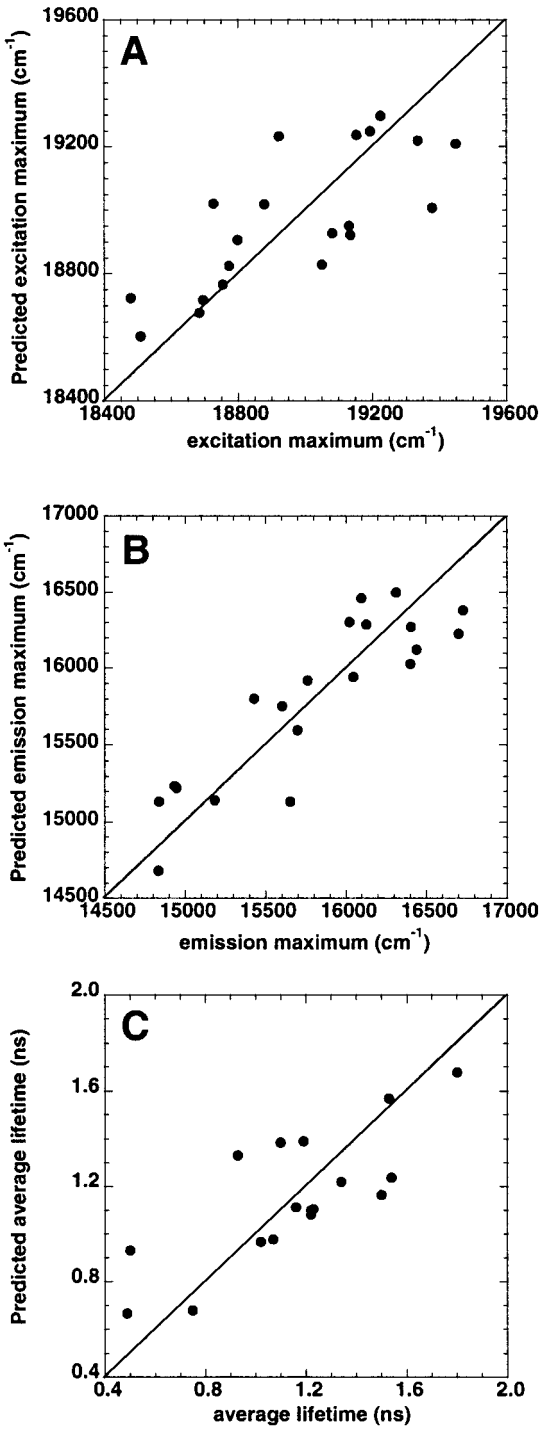

Figure 2. Linear solvation energy relationships for the fluorescence of 7-aminoactinomycin D in various solvents. Plots of predicted vs actual (A) excitation maximum, (B) emission maxium, and (C) fluorescence lifetime are shown. Solvent parameters are given in Table 1. The resulting linear relationships are given by eqs 3−5 in the text.

the sensitivity coefficients for hydrogen bond donation (HBD), hydrogen bond acceptance (HBA), and polarity/polarizability parameters of the solvents used. The Kamlet−Taft equation is, for our case

$$p_i = p_0 - a\alpha_i - b\beta_i - s\pi_i, \qquad (2)$$

where p_i equals the measured property value for different solvents, p_0 is the property in the absence of solvent interaction (i.e., gas phase); α_i is the HBD strength of the solvent; β_i is the HBA strength of the solvent; and π_i is polarity/polarizability parameter of solvent. These parameters have been tabulated for 170 solvents.[20] The solvents chosen here allowed the range of 0.0 to 1.0 for each parameter to be reasonably sampled. Multivariate regression analysis was performed to determine *a*, *b*, and *s* using JMP 3.1 (SAS Institute, Cary, NC). Additionally, the fluorescence properties of 7AAMD were measured in D_2O, C_2D_5OD, and C_6D_6.

Electronic Structure Calculations. The electron density in the ground state of 7AAMD was performed using the semiempirical molecular orbital calculation software MOPAC93 (QCPE program 689; reviewed in [31]). The PM3 Hamiltonian was used for calculations of molecular orbitals.[30] The structure of 7AAMD was constructed by replacing the 7-hydrogen position in the crystal structure of AMD (bound to duplex DNA; [13]) with a 7-amino group. The pentapeptide groups of the drug do not physically interact with the phenoxazone ring chromophore, and hence for the sake of calculations, the peptide atoms beyond the threonine residue were truncated and capped (see Figure 3). The geometry of the molecule was otherwise maintained as in the crystal structure.

The lowest energy excited state was calculated using the multielectron configuration interaction (MECI) scheme within MOPAC. The MECI calculation used the HOMO, LUMO, and the three orbitals above and below these orbitals. Only the ground state and single electron transitions were considered, giving a total of 33 configurations. Visualization of the total electron density of 7AAMD in the ground state and the shift in electron density in the first singlet excited state was performed with the program DENSITY (QCPE 492), slightly modified to allow the large number of occupied orbitals in 7AAMD to be included properly.

Results

Solvatochromism of Excitation Spectra and Stokes Shift. In contrast to actinomycin D, which shows little change in absorbance maximum upon binding to DNA, 7AAMD shows a pronounced shift of the maximum from ~505 nm for the drug in aqueous buffer to ~525 nm for bound drug.[39] This corresponds to a shift in the excitation maximum of the drug as well (Table 1), although the peaks for excitation maxima in water and bound to DNA are slightly different than those of the absorbance (514 and 554 nm, respectively). This may be due to two singlet transitions in the absorbance spectrum of 7AAMD at these wavelengths, as has been reported earlier [34] (see also molecular orbital calculations below), or the presence of tautomeric forms of the drug with different solvent interactions. The former explanation would suggest that excitation of 7AAMD is primarily from the longer-wavelength transition, which for AMD has been attributed to the quinoid ring of the molecule.[1,34]

It is expected, then, that solvent effects would be observed in the excitation spectra of 7AAMD, as well as the usual effect on the Stokes shift. The steady-state fluorescence properties of 7AAMD in 20 solvents are listed in Table 1. The linear free energy relationships derived for excitation maximum and emission maximum are shown in Figure 2A and 2B. For excitation maximum, the relationship determined was (Figure 2A)

$$\hat{\upsilon} = 19376.0 + 298.8\alpha - 909.7\beta \ [\mathrm{cm}^{-1}], \ r^2 = 0.574, \quad p = 0.003 \qquad (3)$$

There was no statistical contribution from π. Equation 3 reveals

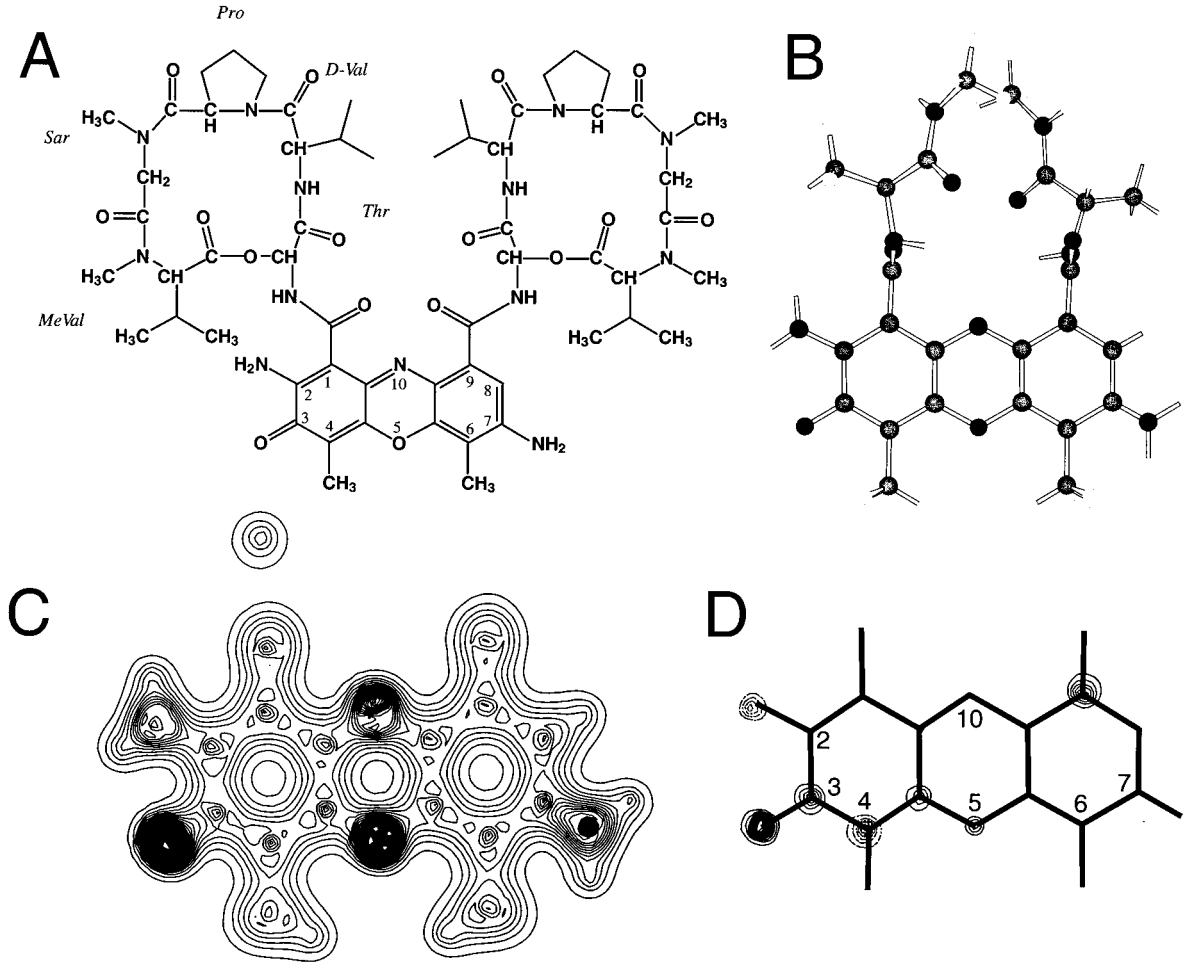

Figure 3. The structure of 7-aminoactinomycin D. (A) the chemical structure of the compound. (B) The truncated 3-dimensional structure used for molecular orbital calculations. (C) Contour plot of the ground-state electron density of the compound as determined from molecular orbital calculations using the structure in (B). (D) Contour plot of the shift of electron density in the first singlet excited state as calculated from configuration interaction calculations. Increased electron density is indicated by solid contours while decreased density is indicated by dashed contours.

TABLE 1: Solvatochromism of 7-Aminoactinomycin D Fluorescence Properties

solvent	excitation maximum (cm^{-1})	excitation width (cm^{-1})	emission maximum (cm^{-1})	emission width (cm^{-1})	Stokes shift (cm^{-1})	π^a	α^a	β^a
DMSO	18 508.6	3640.2	15 698.4	1824.3	2810.2	1.00	0	0.76
DMF	18 685.2	3325.3	15 605.9	2063.6	3079.3	0.88	0	0.69
Methanol	18 878.6	3994.4	14 840.4	2153.1	4038.2	0.60	0.98	0.66
Ethanol	18 799.3	3959.1	14 947.7	2184.8	3851.6	0.54	0.86	0.75
Butanol	18 773.4	3880.5	14 936.4	2369.1	3837.0	0.47	0.84	0.84
Propanol	18 753.8	4023.4	15 183.3	1966.1	3570.5	0.52	0.84	0.90
Acetonitrile	19 378.8	3696.8	15 762.6	2490.1	3616.2	0.75	0.19	0.40
Benzene	19 152.9	3678.4	16 096.6	2557.9	3056.3	0.59	0	0.10
Toluene	18 923.6	3252.3	16 311.3	2458.9	2612.4	0.54	0	0.11
Ethyl acetate	19 134.2	3300.4	16 701.4	2002.9	2432.9	0.55	0	0.45
Butyl acetate	19 081.6	3489.7	16 024.3	2437.6	3057.3	0.46	0	0.45
Acetone	19 131.9	3415.2	16 400.9	2151.0	2731.1	0.71	0.08	0.43
Dichlorethane	19 335.3	2517.9	16 402.9	1911.6	2932.4	0.81	0	0.10
Triethylamine	18 695.5	3353.8	16 728.8	2235.8	1966.8	0.14	0	0.71
Tetrahydrofuran	19 050.3	3224.7	16 437.7	2278.3	2612.6	0.58	0	0.55
Pyridine	18 478.8	3448.5	15 430.5	1966.3	3048.4	0.87	0	0.64
Chloroform	19 226.3	3669.6	16 126.1	2490.0	3100.3	0.58	0.20	0.10
Acetate	19 193.9	3623.0	15 652.8	3535.4	3541.1	0.64	1.12	0.45
Nitrobenzene	18 726.7	4261.0	16 045.2	2391.0	2681.5	1.01	0	0.30
Water	19 448.7	4782.0	14 833.0	2167.5	4615.6	1.09	1.17	0.47
calf thymus DNA	18 050.9	3066.2	15 374.0	1896.0	2677.0	0.59[b]	0.21[b]	0.96[b]
HP1hairpin DNA	18 063.9	3082.8	15 514.1	1913.3	2549.8	0.59[b]	0.17[b]	0.94[b]

[a] Values of α, β, and π from reference (20). [b] Estimated from linear solvation energy relationship.

that the excitation maximum is shifted to shorter wavelengths by HBD solvents and to longer wavelengths by HBA solvents.

Typically, the Stokes shift of fluorescence is affected by the electronic properties of the solvent environment of the fluoro-

TABLE 2: Fluorescence Polarization and Lifetimes for 7-Aminoactinomycin D in Selected Solvents

solvent	polarization	τ (ns)
Cyclohexane	0.243	1.07
Pyridin	0.198	1.53
Toluene	0.164	1.23
Benzene	0.177	1.22
Nitrobenzene	0.425	0.37
Methanol	0.275	0.50
Ethanol	0.251	1.22
Propanol	0.316	1.34
Butanol	0.335	1.50
Isopropyl acetate	0.184	1.04
Butyl acetate	0.203	1.10
Triethylamine	0.190	0.62
Chloroform	0.183	1.02
Dichlorethane	0.212	1.16
Ethyl acetate	0.142	1.19
Acetonitril	0.097	1.54
Acetate	0.359	0.49
DMSO	0.222	1.8[†]
Acetone	0.132	0.93
Water	0.290	0.75[†]
D_{2O}	0.216	1.08[†]

[†] Measured directly via phase modulation. Estimated error from the technique is ± 0.2 ns. All other lifetime values calculated from the Levshin-Perrin equation (see text).

phore. The Stokes shifts are reported in Table 1 but because in our case the excitation maximum is affected by solvent, a more instructive analysis of the LSER is for the emission maximum. The emission LSER is given in Figure 2B, and results in the equation

$$\hat{v} = 17\,055.1 - 869.2\pi - 911.0\,\alpha - 773.6\beta\ [\mathrm{cm}^{-1}],\quad r^2 = 0.777,\ p < 0.0001 \quad (4)$$

As expected, the polarization properties (π) of the solvent influence the emission maxima and contributions are almost equal for π, α, and β. Hence, a shift to shorter wavelengths upon drug transfer from aqueous solution to DNA could result from an environment with decreased polarizability, decreased HBD strength, or decreased HBA strength.

The fluorescence intensity of 7AAMD from 550 to 750 nm was also measured in deuterated solvents. Emission intensity at the emission maximum was increased 3-fold by substitution of H_2O by D_2O, and by 50% in C_2D_5OD vs C_2H_5OH. No change in intensity was observed upon replacing benzene with C_6D_6. These data indicate that 7AAMD forms a hydrogen bond in the excited state. Replacement of H_2O with D_2O in the presence of saturating amounts of the HP1 hairpin DNA resulted in a 2-fold increase in 7AAMD fluorescence intensity as compared to 3-fold for the drug in D_2O alone. This suggests reduced quenching by the solvent for the 7AAMD in the drug−DNA complex compared to free drug. These results are in good agreement with previously reported D_2O-induced changes for 7AAMD bound to calf thymus DNA and nuclei of fixed Chinese hamster ovary cells.[27]

Solvatochromism of Fluorescence Lifetimes. The fluorescence lifetime data for 7AAMD in 20 solvents are given in Table 2. Phase lifetimes were determined directly by the phase modulation technique in DMSO, H_2O, and D_2O, and were calculated from the polarization data in other solvents. Hence, these data reflect average phase lifetimes. Previously, we had determined (from phase and modulation analysis) that 7AAMD has two lifetimes in both aqueous solution and bound to ssDNA (0.4 and 1.9 ns). However, the relative contribution from each is shifted when the drug is bound to the ssDNA.[39] This would result in a measured average lifetime of 0.9 ns in water and 1.7 ns bound to HP1. This is in agreement with the experimentally determined average values of 0.8 ns and 1.7 ns determined by the phase technique alone (Table 2).

A LSER for average fluorescence lifetime could also be established (Figure 2C), where *s*, *a*, and *b* now have units of ns. Nitrobenzene and triethylamine were excluded from the solvent set because their quenching effect on fluorescence is largely through electron transfer.[44,10] The resulting equation for the dependence of lifetime on solvent parameters is

$$\tau = 0.98 - 0.65\,\alpha + 0.84\beta\ [\mathrm{ns}],\ r^2 = 0.596,\ p = 0.007 \quad (5)$$

There was no statistical contribution from π. Hence, the lifetimes are decreased in HBD solvents and increased in HBA solvents. Because the quenching of fluorescence by HBD solvents could be due to proton transfer in the excited state (see, e.g., ref 19), we measured directly the lifetime of 7AAMD in aqueous solution at pH 3.0, 7.0, and 10.0. No change in the average lifetime was observed over this pH range, suggesting no proton transfer in the excited state. We also observed an increase of lifetime in D_2O vs H_2O (1.1 ns vs 0.8 ns). This accounts for the increase in fluorescence emission intensity noted above for deuterated solvents, and suggests hydrogen bonding between 7AAMD in solvent during the excited state. Hydrogen bond donation from solvent results in coupling of the 7AAMD excited state to the H−O− vibration of the solvents, and hence vibronic quenching of the excited state.[35] Therefore, the increased fluorescence intensity upon 7AAMD binding to HP1 likely reflects reduced water access to the chromophore in the bound state rather than a major change in the polarization of the environment of the drug (it is unlikely that any region of DNA has a significantly higher HBA property than bulk water).

Calculations of the Electronic Excited State of 7AAMD. Using semiempirical molecular orbital methods, the electronic structure of the ground and lowest singlet excited state could be calculated. Figure 3B describes the truncated form of 7AAMD used for the calculations. The total electron density of 7AAMD in the ground state is shown in Figure 3C as a contour plot of the plane of the phenoxazone ring. The regions of highest electron density are primarily localized to O5, N10, and the quinoid carbonyl oxygen on C3 of the phenoxazone ring.

The excited states of 7AAMD were calculated with multi-electron configuration interaction. The calculated transition wavelengths and oscillator strengths for singlet transitions are given in Table 3. Upon excitation to the lowest energy singlet state ($S_0 \rightarrow S_1$), the change in electron density is shown in Figure 3D as a contour plot. The solid black contours represent gain of density while the dashed contours represent loss of density. The predominant transition of density is an increase on the quinoid carbonyl at C3 with a loss on the amino group at C2. There is also a slight gain of density at C9 in the benzenoid portion of the ring. The calculated transition wavelength of 498 nm is in good agreement with the experimental absorption maximum of 505 nm and the gas-phase excitation wavelength of 516 nm (determined from eq 3). The second lowest energy transition ($S_0 \rightarrow S_2$) is calculated to be at 412 nm, and hence, the absorbance spectrum of 7AAMD contains two overlapping transitions in the 400−600 nm region.

Discussion

We have used linear solvation energy relationships for the solvatochromism of the fluorescence properties of 7AAMD to

TABLE 3: Calculated Singlet Excited State Transitions and Oscillator Strengths for 7-Aminoactinomycin D

transition	transition wavelength (nm)	oscillator strength
$S_0 \rightarrow S_1$	498	1.032
$S_0 \rightarrow S_2$	412	0.266
$S_0 \rightarrow S_3$	361	0.274
$S_0 \rightarrow S_4$	357	0.005
$S_0 \rightarrow S_5$	315	0.077
$S_0 \rightarrow S_6$	293	0.004
$S_0 \rightarrow S_7$	263	0.827
$S_0 \rightarrow S_8$	246	0.004
$S_0 \rightarrow S_9$	234	0.238
$S_0 \rightarrow S_{10}$	226	0.087
$S_0 \rightarrow S_{11}$	218	0.018
$S_0 \rightarrow S_{12}$	209	0.000
$S_0 \rightarrow S_{13}$	185	0.000
$S_0 \rightarrow S_{14}$	177	0.001
$S_0 \rightarrow S_{15}$	172	0.000
$S_0 \rightarrow S_{16}$	152	0.000

determine why the fluorescence emission spectrum of the drug is substantially blue shifted and quantum yield increased on binding of the drug to a DNA hairpin containing a high affinity site for the drug (Figure 1). It was our hope that the unique fluorescence signature could be used to understand why the drug has such an affinity for this DNA secondary structure, and particularly, that novel agents might be designed to take advantage of any unique physical chemical environment found in DNA hairpins but not in duplex, double stranded, Watson−Crick form DNA.

Our solvatochromism data for 7AAMD yield a fairly straightforward interpretation: fluorescence excitation is red shifted from that observed in aqueous solution by an environment with reduced hydrogen bond donating capabilities and increased hydrogen bond accepting capability. Fluorescence emission is blue shifted relative to aqueous solution by an environment that is reduced in all three parameters relative to water: polarization, hydrogen bond donation, and hydrogen bond accepting. Fluorescence lifetimes are shortened in an environment of hydrogen bond donation and increased by an environment with hydrogen bond acceptance.

Our calculations of the electronic excited states of 7AAMD aid in explaining the solvatochromism of fluorescence. The lowest energy singlet transition for 7AAMD leads to an increase in electron density on the carbonyl oxygen of the quinoid portion of the 7AAMD phenoxazone ring. This increased negative charge results in an enhanced interaction with protons of the solvent molecules available for hydrogen bonding, and is likely responsible for vibronic coupling of the molecule to H−O− vibrations.

These data are all consistent with a theoretical model of 7AAMD bound to the HP1 complex reported earlier.[41] This model is shown in detail in Figure 4. Through nuclease mapping, a structure for HP1 was determined that included an unusual tandem of an A•G mismatch followed by a T•T mismatch. Because guanine is required for DNA binding, the 7AAMD can be positioned into an intercalation site on HP1 where the quinoid oxygen at C3 of 7AAMD (the one carrying enhanced negative charge in the first excited state; lower arrow in Figure 4 is surrounded by the 5-methyl group of thymidine above it (upper arrow in Figure 4), its own C4-methyl group on one side, and the deoxyribose sugar of adenine residue 19 on the other side. This binding mode thus reveals a hydrophobic "pocket" within which the 7AAMD is located and shielded from solvent (and hence its quenching effect). Consequently, this gives rise to the increased fluorescence intensity, increased fluorescence lifetime, and blue shift of the emission maximum.

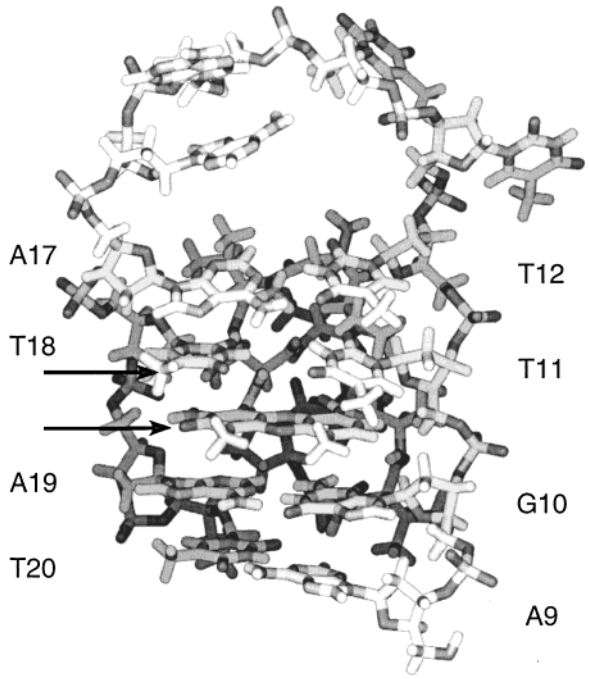

Figure 4. Molecular model of 7-aminoactinomycin D bound to the DNA hairpin HP1 (see text for DNA sequence). The construction of this model is described in ref 41. The bound drug is located in an intercalation site with phenoxazone oxygen of carbon 3 located in a hydrophobic pocket (indicated by lower arrow). This oxygen gains electron density in the excited state (see Figure 3). The location of the 5-methyl group of thymidine 18 (upper arrow), along with the 4-methyl group of 7-aminoactinomyin D and the deoxyribose ring of adenine 19 protect the drug from solvent-mediated fluorescence quenching.

This model suggests that hydrophobic "matching" of 7AAMD to specific regions within the binding site is responsible for the increased affinity of 7AAMD for this site vs similar sites on double-stranded, Watson−Crick DNA. Hence, matching of hydrophobic sites, in addition to appropriate hydrogen bonding, are important considerations for development of novel compounds able to target DNA secondary structures, such as the HP1 hairpin used here. Such interactions increase the binding affinity over the stacking and hydrogen bonding interactions usually associated with intercalating, DNA-binding ligands (e.g., refs 2 and 21). Novel hairpin-binding ligands that exploit this additional binding free energy source are now under development in our laboratories.

Acknowledgment. The model in Figure 4 was constructed by Chang-Shung Tung, Los Alamos National Laboratory as detailed in ref 41. This work was partially supported by Grant No. RB2-2031 from the Civilian Research and Development Foundation (CRDF), Arlington, Virginia, USA.

References and Notes

(1) Auer, H. E.; Pawlowski-Konopnicki, B. E.; Chiao, Y.-C. C.; Krugh, T. R. *Biopolymers* **1978**, *17*, 1891−1911.

(2) Chaires, J. B. *Curr. Opinion Struct. Biol.* **1998**, *8*, 314−320.

(3) Chiao, Y.-C.; Rao, K. G.; Hook, J. W.; Krugh, T. R.; Sengupta, S. K. *Biopolymers* **1979**, *18*, 1749−1762.

(4) Davis, W. R.; Gabbara, S.; Hupe, D.; Peliska, J. A. *Biochemistry* **1998**, *37*, 14 213−14 221.

(5) Gill, J. E.; Jotz, M. M.; Young, S. G.; Modest, E. J.; Sengupta, S. K. *J. Histochem. Cytochem.* **1975**, *23*, 793−799.

(6) Goldberg, I. H.; Beerman, T. A.; Poon, R. Antibiotics: Nucleic Acids as Targets in Chemotherapy. In *Cancer 5*: *A Comprehensive Treatise*; Becker, F. F., Ed.; Plenum: New York, 1977; pp 427−456.

(7) Goldberg, I. H.; Friedman, P. A. *Annu. Rev. Biochem.* **1971**, *40*, 775−810.
(8) Graves, D. E.; Wadkins, R. M. *J. Biol. Chem.* **1989**, *264*, 7262−7266.
(9) Guo, J.; Wu, T.; Bess, J.; Henderson, L. E.; Levin, J. G. *J. Virology* **1998**, *72*, 6716−6724.
(10) Inada, T. N.; Kikuchi, K.; Takahashi, Y.; Ikeda, H.; Miyashi, T. *J. Photochem. Photobiol. A* **2000**, *137*, 93−97.
(11) Jares-Erijman, E. A.; Klement, R.; Machinek, R.; Wadkins, R. M.; Kankia, B. I.; Marky, L. A.; Jovin, T. M. *Nucleosides & Nucleotides* **1997**, *16*, 661−667.
(12) Jeeninga, R. E. *Nucleic Acids Res.* **1998**, *26*, 5472−5479.
(13) Kamitori, S.; Takusagawa, F. *J. Mol. Biol.* **1992**, *225*, 445−456.
(14) Kamlet, M. J. *Prog. Phys. Chem. Org. Chem.* **1993**, *19*, 295−317.
(15) Kamlet, M. J.; Taft, R. W. *J. Chem. Soc., Perkins Trans.* **1979**, *2*, 337−341.
(16) Kamlet, M. J.; Taft, R. W. *Acta Chem. Scand. B* **1985**, *39*, 611−628.
(17) Kersten, H.; Kersten, W. Actinomycin. In *Inhibitors of Nucleic Acid Synthesis*; Springer: Berlin, 1974; pp 40−66.
(18) Lakowicz, J. R. *Principles of Fluorescence Spectroscopy*; Plenum Press: New York, 1983.
(19) Laws, W. R.; Brand, L. *J. Phys. Chem.* **1979**, *83*, 795−802.
(20) Marcus, Y. *Chem. Soc. Rev.* **1993**, *22*, 409−416.
(21) Marky, L. A.; Snyder, J. G.; Remeta, D. P.; Breslauer, K. J. *J. Biomolec. Struct. Dyn.* **1983**, *1*, 487−507.
(22) *Brief Handbook of Physico-Chemical Data*; Mischenko, K. P., Ravdel, A. A., Eds.; Chemistry Publishers (in Russian): Leningrad, 1974.
(23) Modest, E. J.; Sengupta, S. K. *Cancer Chemother. Rep.* **1974**, *58*, 35−48.
(24) Müller, W.; Crothers, D. M. *J. Mol. Biol.* **1968**, *35*, 251−290.
(25) *Handbook of Chemistry*; Nikolski, B. P., Ed.; Chemistry Publishers (in Russian): Moscow, 1965.
(26) Rill, R. L.; Hecker, K. H. *Biochemistry* **1996**, *35*, 3525−3533.
(27) Sailer, B. L.; Nastasi, A. J.; Valdez, J. G.; Steinkamp, J. A.; Crissman, H. A. *J. Histochem. Cytochem.* **1997**, *45*, 165−175.
(28) Sha, F.; Chen, F.-M. *Biophys. J.* **2000**, *79*, 2095−2104.
(29) Sobell, H. M. *Proc. Natl. Acad. Sci. U.S.A.* **1985**, *82*, 5328−5331.
(30) Stewart, J. J. P. *J. Comput. Chem.* **1989**, *10*, 221−264.
(31) Stewart, J. J. P. *J. Computer-aided Mol. Design* **1990**, *4*, 1−105.
(32) Straney, D. C.; Crothers, D. M. *Biochemistry* **1987**, *26*, 1987−1995.
(33) Taft, R. W.; Abboud, J.-L. M.; Kamlet, M. J.; Abraham, M. H. *J. Solution Chem.* **1985**, *14*, 153−175.
(34) Tai, J. C.; Craig, W. S.; Gaber, B. P. *J. Am. Chem. Soc.* **1976**, *98*, 7925−7927.
(35) Vekshin, N. L. *Photonics of Biopolymers*; Moscow State University Press: Moscow, 1999.
(36) Verweij, J.; Schellens, J. H. M.; Loo, T. L.; Pinedo, H. M. Antitumor Antibiotics. In *Cancer Chemotherapy and Biotherapy, 2nd ed.*; Chabner, B. A., Longo, D. L., Eds.; Lippincott−Raven Publishers: Philadelphia, 1996; pp 395−407.
(37) Wadkins, R. M. *Curr. Med. Chem.* **2000**, *7*, 1−15.
(38) Wadkins, R. M.; Jares-Erijman, E. A.; Klement, R.; Rüdiger, A.; Jovin, T. M. *J. Mol. Biol.* **1996**, *262*, 53−68.
(39) Wadkins, R. M.; Jovin, T. M. *Biochemistry* **1991**, *30*, 9469−9478.
(40) Wadkins, R. M.; Tung, C.-S.; Vallone, P. M.; Benight, A. S. *Arch. Biochem. Biophys.* **2000**, *384*, 199−203.
(41) Wadkins, R. M.; Vladu, B.; Tung, C.-S. *Biochemistry* **1998**, *37*, 11 915−11 923.
(42) Waring, M. J. *Annu. Rev. Biochem.* **1981**, *50*, 159−162.
(43) White, R. J.; Phillips, D. R. *Biochemistry* **1988**, *27*, 9122−9132.
(44) Zander, M.; Breymann, U.; Dreeskamp, H.; Koch, E. *Z. Naturforsch. A* **1977**, *32A*, 1561−1563.